

Received February 21, 2019, accepted March 14, 2019, date of publication March 27, 2019, date of current version April 13, 2019.

Digital Object Identifier 10.1109/ACCESS.2019.2907723

Wideband Linearly-Polarized and Circularly-Polarized Aperture-Coupled Magneto-Electric Dipole Antennas Fed by Microstrip Line With Electromagnetic Bandgap Surface

JIE SUN¹, (Student Member, IEEE), AND KWAI-MAN LUK², (Fellow, IEEE)

State Key Laboratory of Terahertz and Millimeter Wave, City University of Hong Kong, Hong Kong

Department of Electronic Engineering, City University of Hong Kong, Hong Kong

Corresponding author: Jie Sun (sunjie1106@gmail.com)

This work was supported by the Research Grant Council of Hong Kong, China, under Project 9042674 (CityU 11217618).

ABSTRACT Wideband aperture-coupled magneto-electric (ME) dipole antennas fed by microstrip line are proposed in this paper. The aperture-coupled microstrip-line-fed method was utilized in the proposed configuration to replace the conventional Γ -shaped probe to excite the ME dipole antenna. Particularly, a printed mushroom-like electromagnetic bandgap (EBG) surface was mounted below the microstrip line to effectively eliminate the back radiation caused by the aperture on the ground plane. Two configurations of ME dipole antennas with linear polarization (LP) and circular polarization (CP) have been proposed for adequately studying the effect of the EBG surface. Both the simulation and measurement of the two prototypes had been carried out for verification. Based on the measured results, wide impedance bandwidth ($SWR < 2$) of 54.9% and 58% can be obtained for both the proposed LP and CP ME dipole antennas, respectively. Besides, the performances of the stable broadside radiation pattern with the enhanced front-to-back ratio (FBR) can also be achieved for both configurations.

INDEX TERMS Aperture-coupled, microstrip line, magneto-electric (ME) dipole, linearly-polarized antenna, circularly-polarized antenna, electromagnetic bandgap (EBG) surface.

I. INTRODUCTION

Wideband antennas always exhibit very competitive performances since they can provide larger channel capacities for covering multiple alternative spectrums simultaneously, which is particularly crucial for fifth generation (5G) wireless communication systems [1]. Due to the low-profile structure, low cost, easy to be fabricated and lightweight features, wideband patch antennas have been widely investigated over past few decades with various invented advanced methods, including U-slot patches, stacked patches, E-shaped patch, L-shaped probe-fed patch, parasitic elements, multiple resonance modes and so on [3]–[7]. Although the impedance bandwidth can be enhanced over 30%, the high cross-polarizations and unstable gain performance still affect their practical applications. Reflector-backed dipoles are another widely used antennas due to its simple construction [8]–[10].

The associate editor coordinating the review of this manuscript and approving it for publication was Yejun He.

Basically, the bandwidth of dipole is intrinsically narrow. By employing some advanced structure, the bandwidth can be enhanced. However, the beamwidth or gain are not very stable over wide operating frequencies, and the E-plane and H-planes are not very symmetrical to each other [11], [12].

Magneto-electric (ME) dipole antenna is a novel kind of wideband complementary antenna proposed in 2006 [13]. By combination of an electric dipole and a magnetic dipole together, very wide bandwidth of over 50% can be easily obtained. Usually, a Γ -shaped probe is utilized as the feeding portion to ensure a wide bandwidth [13], [14]. However, the antenna performance is very sensitive to the dimensions of the Γ -shaped probe, which greatly increases the machining complexity and cost of fabrication, especially for the practical massive production. Besides, the Γ -shaped probe is quite difficult to be fulfilled at millimeter-wave frequencies for the 5G applications. The aperture-coupled method is a preferable way to simplify this feeding portion and has been successfully realized when the substrate integrated waveguide

TABLE 1. Dimension of the proposed structure of aperture-coupled ME dipole antennas.

| Parameter | L_1 | L_2 | W_1 | W_2 | G | L_{EBG} | G_{EBG} | D_{EBG} |
|-----------|-------|-------|-------|-------|-----|-----------|-----------|-----------|
| Value(mm) | 41 | 16 | 3 | 4.5 | 100 | 8 | 1.5 | 1 |

(SIW) is utilized as the feed at millimeter-wave frequencies [15], [16]. For the microwave applications, the microstrip line or stripline is a more practical and convenient choice than SIW, and had been proposed in [17], [18]. However, the backlobes in [17] appear quite larger due to the aperture on the ground plane when using microstrip-line-fed method. Stripline surrounded by rows of metalized plated-through-holes can reduce the backward radiation among some partial bandwidth [18]. However, for antennas with larger bandwidth, the effect of stripline may seriously become degraded at upper frequencies [18]. Also, all the metalized plated-through-holes need to be implemented through multiply printed circuit boards (PCB), which increase the total fabrication cost and complexity.

In this paper, wideband aperture-coupled ME dipole antenna fed by microstrip line backed with electromagnetic bandgap (EBG) surface is proposed. A printed EBG structure has been mounted below the aperture. Basically, the EBG layer can be considered as a high impedance surface to effectively suppress the unwanted surface waves and parallel-plate waveguide mode caused by backward radiation from the aperture within its frequencies of bandgap [19]–[23]. The bandgap can be designed wide enough to cover the entire impedance bandwidth of proposed ME dipole antennas. Thus, the back radiation can be eliminated over the whole operating frequencies. Furthermore, the whole feeding structure can be firstly realized on each single PCB layer and then be attached together, which avoids the complex process of via-holes through different PCB layers in stripline and can also be realized at millimeter-wave bands for the 5G application. For verifying the effect of the EBG structure, two configurations of aperture-coupled ME dipole antennas with linear polarization (LP) and circular polarization (CP) are designed and proposed, respectively. The results demonstrate that both the aperture-coupled LP and CP ME dipoles can achieve a wide impedance bandwidth of more than 50% with the enhanced front-to-back ratio across the entire operating bands.

The paper is organized as follows. The antenna geometry is described in Section II. The working principle is illustrated in Section III. The discussion on the EBG surface is given in Section IV. The simulated and measured performances and discussions are displayed in Section V. Finally, a conclusion in Section VI is given at the end of the paper

II. ANTENNA GEOMETRY DESCRIPTION

The proposed configurations of ME dipole antennas fed by microstrip lines are illustrated in Fig. 1, Fig. 2 and Fig. 3, with detailed parameters shown in Table. 1 and Table. 2. ME dipole antenna is placed at the top position, excited by the aperture etched on the ground plane. Three stacked layers

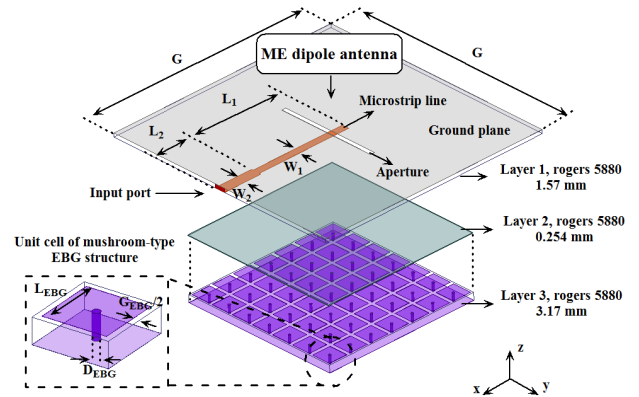


FIGURE 1. Proposed configuration of aperture-coupled ME dipole antennas fed by microstrip line with EBG surface.

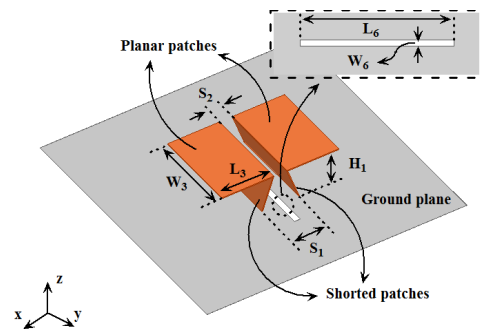


FIGURE 2. Perspective view of the LP ME dipole antenna.

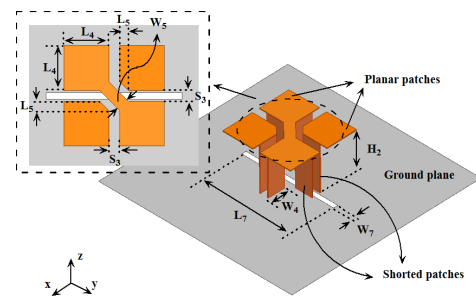


FIGURE 3. Perspective view of the CP ME dipole antenna.

with the same relative dielectric constant of 2.2, are mounted below the top ME dipole antenna. Layer 1 is composed of a ground plane on upper side and a microstrip line with 50 ohm printed on bottom side. A rectangular aperture was etched in the center of the ground plane for coupling the EM waves from the microstrip line to the ME dipole. The microstrip line of 50 ohm characteristic impedance consists of two separate widths w_1 and w_2 due to the existence of partial EBG surface below. The layer 2 is a piece of thin square substrate, offering the indispensable gap between layer 1 and layer 3. A printed mushroom-like EBG structures are implemented on layer 3. The EBG are grounded by conductor plated via holes and the dimension is smaller than ground plane. All three layers are implemented on PCB laminates (Rogers 5880), which is low in fabrication cost and easy to be integrated with other

TABLE 2. Dimension of two ME dipole antennas with linear polarization and circular polarization.

| | | | | | |
|------------|-------|-------|-------|-------|-------|
| Parameter | L_3 | L_4 | L_5 | L_6 | L_7 |
| Value (mm) | 16 | 12.5 | 2.5 | 42 | 38 |
| Parameter | W_3 | W_4 | W_5 | W_6 | W_7 |
| Value (mm) | 26 | 7 | 3.54 | 1.8 | 1.8 |
| Parameter | H_1 | H_2 | S_1 | S_2 | S_3 |
| Value (mm) | 10 | 18 | 11 | 4 | 3 |

electronics. Furthermore, all the PCB layers are independent to each other, so that they can be fabricated separately first, and then be attached together using screws or bonding films.

A. LINEARLY-POLARIZED ME DIPOLE ANTENNA

The linearly-polarized ME dipole antenna is shown in Fig. 2 with detailed parameter values displayed in Table. 2. Two rectangular horizontal patches serve as a planar electric dipole. Two tilted shorted patches and the middle ground plane between them forms a triangular current loop, regarded as the magnetic dipole. A ground plane is placed below the ME dipole for obtaining a unidirectional radiation pattern.

B. CIRCULARLY-POLARIZED ME DIPOLE ANTENNA

The circularly-polarized ME dipole antennas is plotted in Fig. 3 with detailed dimensions shown in Table. 2. Four horizontal patches contribute to the planar electric dipole. The vertically shorted patches and ground plane form the magnetic dipole. For exciting a circular polarization, a metallic strip is used in this structure to connect two horizontally oriented patches at the diagonal position [16].

III. ANTENNA WORKING PRINCIPLE

The ME dipole is a type of inherently complementary antenna consisting of an electric dipole and magnetic dipole. To clearly determine its operating principle, both the current and electric field distributions need to be studied. The current distribution on two horizontal patches represents the working state of electric dipole, while the electric field strength over the middle aperture represents the working state of the magnetic dipole.

For the LP ME dipole antenna, the current distributions on two horizontal patches and the electric field distributions across the aperture at center frequency of 4.7 GHz over one period of time are studied, with detailed simulated results shown in Fig. 5. Since ME dipole is a complementary antenna, both the electric dipole and magnetic dipole are excited in phase simultaneously over one period of time. In Fig. 5, when at time $t = 0$ and $T/2$ where T corresponds to one period of time, the magnitude of both current and electric field turn out very weak. When at time $t = T/4$ and $3T/4$, the magnitude of current becomes quite strong with a sinusoidal distribution along the x direction. This phenomenon proves that the electric dipole and magnetic dipole are simultaneously excited in phase in a period of

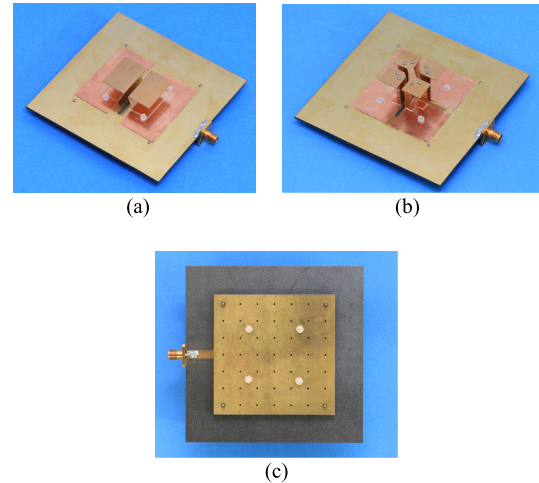


FIGURE 4. Photography of the prototypes for both LP and CP ME dipole antennas fed by the microstrip lines: (a) LP ME dipole antenna, (b) CP ME dipole antenna, (c) bottom view for both LP and CP ME dipole antennas.

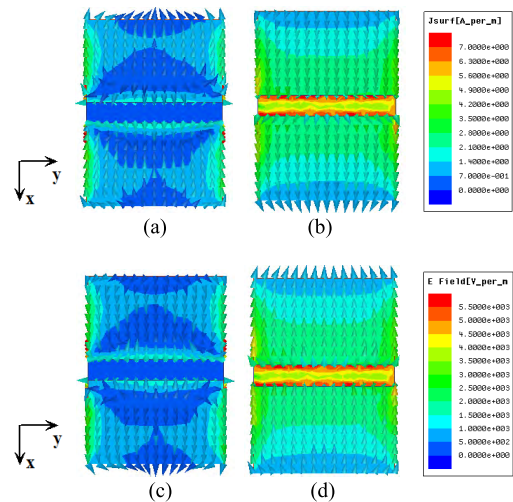


FIGURE 5. Simulated current distributions on the horizontal patches and electric field distributions on the aperture during one period of time for the proposed LP ME dipole antenna at 4.7 GHz. (a) $t = 0$. (b) $t = T/4$. (c) $t = T/2$. (d) $t = 3T/4$.

time, which is coincident to the theory of complementary antenna.

For the CP ME dipole antenna, the current and electric field distributions at center frequency of 4.3 GHz have been shown in Fig. 6. In order to obtain the circular polarization, a commonly used method is to excite two orthogonal linear polarizations with 90° phase difference to each other. In Fig. 6, at time $t = 0$ and $t = T/2$, the current on the horizontal patches are along y direction with sinusoidal distribution, and the electric field across an aperture along x direction are dominated. Thus, at time $t = 0$ and $T/2$, a linear polarization along y direction is mainly excited. Similarly, at time $t = T/4$ and $3T/4$, linear polarization along x direction is strongly excited. The two sets of polarizations are in orthogonal directions with nearly equal amplitude and 90° phase difference, resulting in a circular polarization.

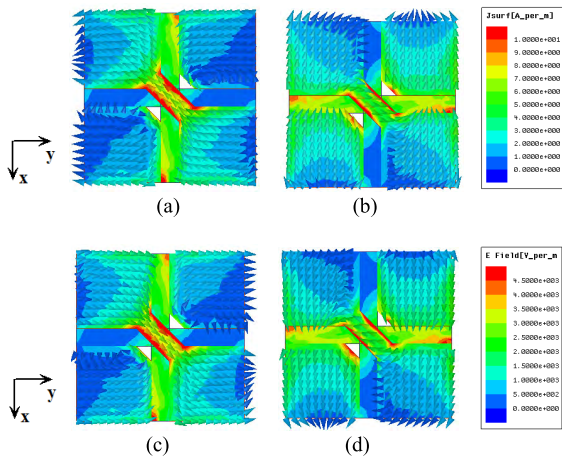


FIGURE 6. Simulated current distributions on the horizontal patches and electric field distributions on the aperture during one period of time for the proposed CP ME dipole antenna at 4.3 GHz. (a) $t = 0$. (b) $t = T/4$. (c) $t = T/2$. (d) $t = 3T/4$.

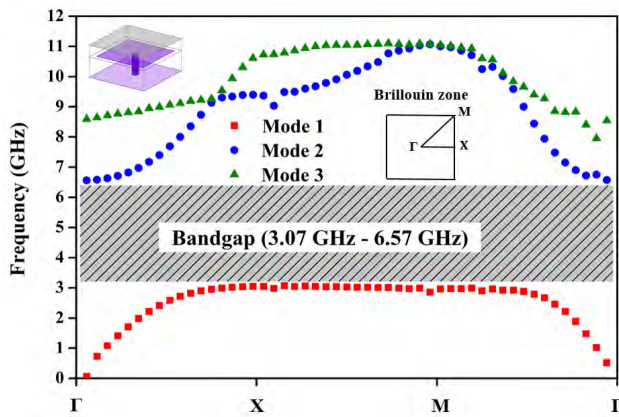


FIGURE 7. Simulated Brillouin diagram for the designed EBG structure.

IV. DISCUSSION ON THE ELECTROMAGNETIC BANDGAP (EBG) SURFACE

When using the aperture-coupled method to excite the ME dipole, the back radiation caused by the aperture usually deteriorate the performance of front-to-back ratio (FBR) and gain. Backing a reflecting plate at a distance of approximately a quarter wavelength is a commonly employed way to alleviate the backlobe [24]. However, it has some drawbacks. Firstly, the distance of a quarter wavelength cannot be accurately guaranteed for the antenna with very wide operating frequencies. Secondly, a quarter wavelength will increase the total height of the antenna, leading into a quite bulky profile. Thirdly, the caused parallel-plate electromagnetic mode between the reflector and the ground plane can also degrade the radiation pattern and efficiency [21], [23].

Mounting a layer of EBG surface below the aperture is a more effective solution to eliminate the unwanted back radiation from the aperture when compared with conventional methods of backing a piece of reflecting plate or incorporating the stripline feeding structure [18], [24]. The EBG surface can generate a stopband. Within the stopband, any directions of electromagnetic wave will not propagate along

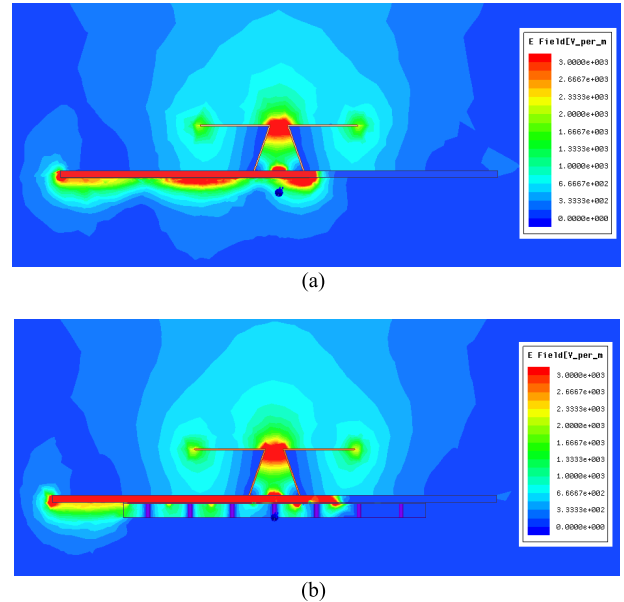


FIGURE 8. Magnitude distribution of electric field on the E-plane at 4.4 GHz (a) without EBG surface, (b) with EBG surface.

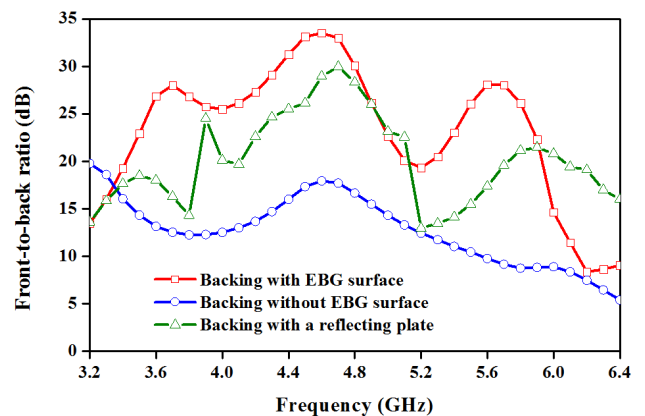


FIGURE 9. Comparison of the simulated front-to-back ratio for the proposed aperture-coupled LP ME dipole antenna fed by microstrip line.

EBG surface, and the parallel-plate electromagnetic mode can be suppressed [19], [20]. The bandgap can be designed to be wide enough for the antenna with a wide impedance bandwidth. The result of simulated bandgap for the EBG surface used in this paper is shown in Fig. 7. Designed stopband covers from 3.07 to 6.57 GHz, which is wide enough for the proposed ME dipole antenna. Furthermore, the height of the EBG structure proposed in this designs are $0.05 \lambda_0$ or $0.07 \lambda_g$ (for LP ME dipole antenna) and $0.045 \lambda_0$ or $0.067 \lambda_g$ (for CP ME dipole antenna), where λ_0 and λ_g refer to the wavelength in the air and substrate, respectively. The height of EBG layer is much smaller than a quarter wavelength ($0.25 \lambda_0$). Thus, the aperture-coupled ME dipole antenna with EBG surface backed has a much lower profile than the aperture-coupled ME dipole antenna backed with a metallic reflecting plate.

The magnitude distributions of electric field in E-plane for LP ME dipole antenna with and without EBG surface is

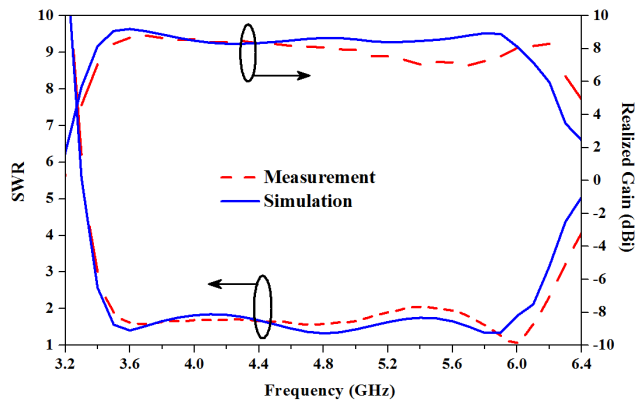


FIGURE 10. Performances SWR and realized gain of the proposed aperture-coupled LP ME dipole antenna fed by microstrip line with the EBG surface.

plotted in Fig. 8. Here, only the LP ME dipole antenna is taken as the example, since the CP ME dipole employs the same feeding structure as the LP ME dipole. When backing an EBG surface below the aperture, the electric field in the backward region decreases considerably, resulting in the weak back radiations. Besides, the performances of simulated FBRs of LP ME dipole backed with or without EBG surface and with a reflecting plate at a quarter wavelength of center wavelength has been studied. The simulated results are given in Fig. 9. It can be seen that by mounting an EBG surface below the aperture, the FBR is enhanced above 20 dB over entire working frequencies. When placing a reflecting plate at a fix distance of a quarter wavelength in terms of the center frequency, the FBR at center frequencies can be improved while the FBR at low and high frequencies are still worse. When nothing backed below the aperture, the FBR only ranges between 10 and 18 dB.

V. ANTENNA PERFORMANCE AND DISCUSSION

Both prototypes of LP and CP ME dipole antennas were fabricated with the simulated and measured performances displayed in this part. The S-parameters were measured by Agilent E5071C network analyzer, while the radiation pattern, gain and axial ratio were tested using the SATIMO complex antenna measurement system.

A. LINEARLY-POLARIZED (LP) ME DIPOLE ANTENNA

The performances of SWR and realized gain are plotted in Fig. 10. The simulated and measured impedance bandwidths with SWR < 2 are 54.5% (from 3.46 to 6.05 GHz) and 54.9% (from 3.5 to 6.15 GHz), which are in good agreement to each other. Three resonances are generated as shown in Fig. 7. The first two resonances are excited by the electric dipole and magnetic dipole, respectively, while the third resonance is excited by the aperture on the ground plane. Thus, the three existing resonances contribute to the wide impedance bandwidth of over 50%. The simulated gain varies from 8.3 to 9.2 dBi, while the measured gain ranges between 7.0 and 8.8 dBi. The difference between the simulation and

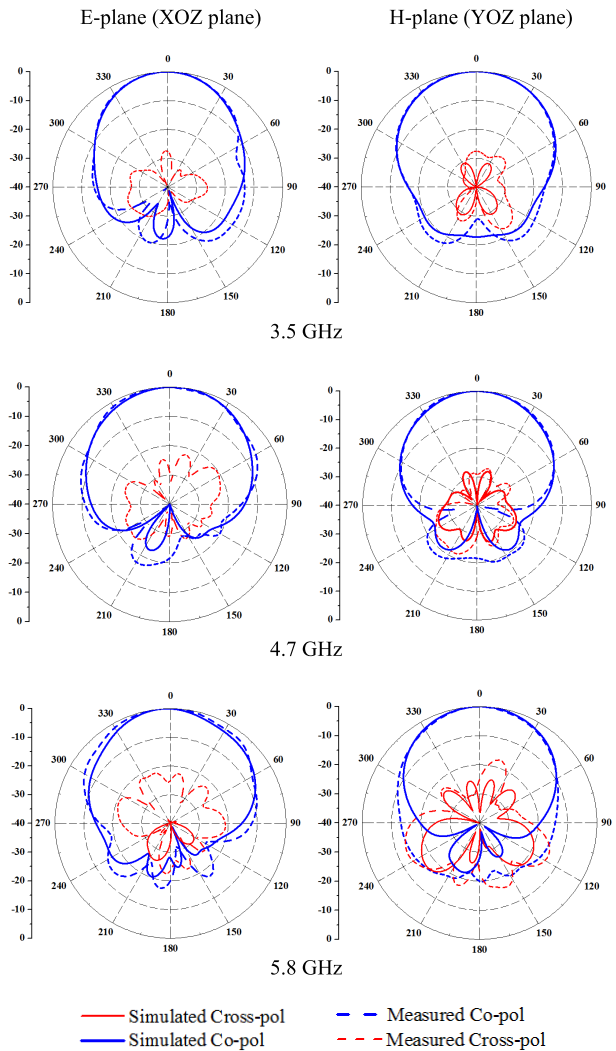


FIGURE 11. Performances of radiation pattern of the proposed LP ME dipole antennas over the operating frequencies.

measurement is mainly due to the fabrication tolerance and measurement system deviation. Besides, since multiple PCB layers are utilized in the proposed structure, the possible tiny air gap sandwiched between any two layers may also cause the drop of the gain at some frequencies.

Fig. 11 demonstrates the performances of both the simulated and measured radiation pattern over entire operating frequencies. Stable broadside radiation patterns with linearly polarization can be achieved for both E-plane and H-plane. The cross-polarization is below -22 dB for almost operating frequencies, except for a small fraction of higher frequencies. The backlobes are below -20 dBi over entire working band. The low back radiation is mainly due to existence of the EBG surface backed below the aperture on the ground plane.

B. CIRCULARLY-POLARIZED (CP) ME DIPOLE ANTENNA

Fig. 12 depicts the simulated and measured SWRs and gains across the whole operating bandwidth of the proposed CP

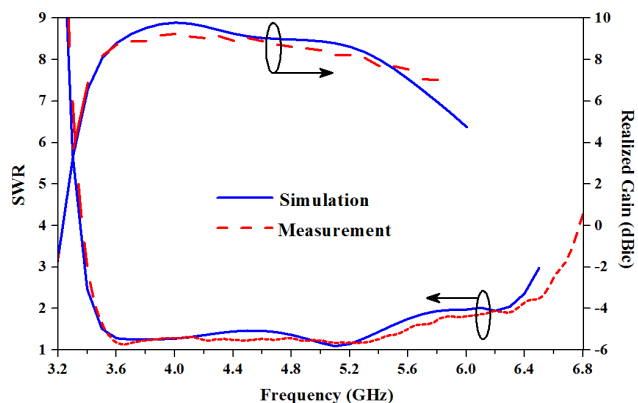


FIGURE 12. Performances of SWR and realized gain of the proposed CP ME dipole antenna fed by microstrip line with the EBG surface.

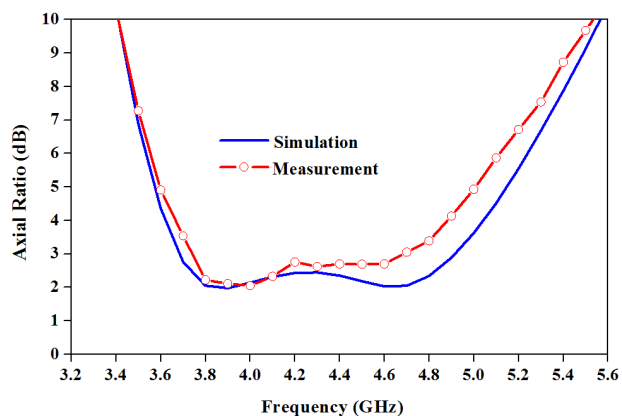


FIGURE 13. Performances of axial ratio bandwidth of the proposed CP ME dipole antenna fed by microstrip line with the EBG surface.

ME dipole antenna. The simulated impedance bandwidth is 58% with $SWR < 2$, from 3.44 to 6.27 GHz, which coincides with the measured impedance bandwidth of 58.2% with $SWR < 2$ from 3.48 to 6.34 GHz. The performance of axial ratio (AR) is shown in Fig. 13. The simulated AR bandwidth ($AR < 3$ dB) is 28.4% from 3.68 to 4.9 GHz, while the measured AR bandwidth is 22.5% from 3.75 to 4.7 GHz. The simulated realized gain over the AR bandwidth varies from 8.9 to 9.8 dBic versus the measured gain in the range from 8.7 to 9.24 dBic, as shown in Fig. 12. The difference between the simulated and measured performances of ARs and gains are due to the fabrication tolerance.

The performances of simulated and measured radiation pattern in two orthogonal planes (H-plane and V-plane) at 3.8, 4.2 and 4.6 GHz are displayed in Fig. 14. The left-hand circular polarization refers to the co-polarizations and the right-hand circular polarization refers to the cross-polarization. It can be revealed that the stable unidirectional radiation patterns with small backlobes and symmetric H- planes and V-planes can be achieved across the whole AR bandwidth. The cross-polarization is below -15 dB over the operating frequencies. The 3-dB AR beamwidth for both H-plane and V-plane are nearly symmetric.

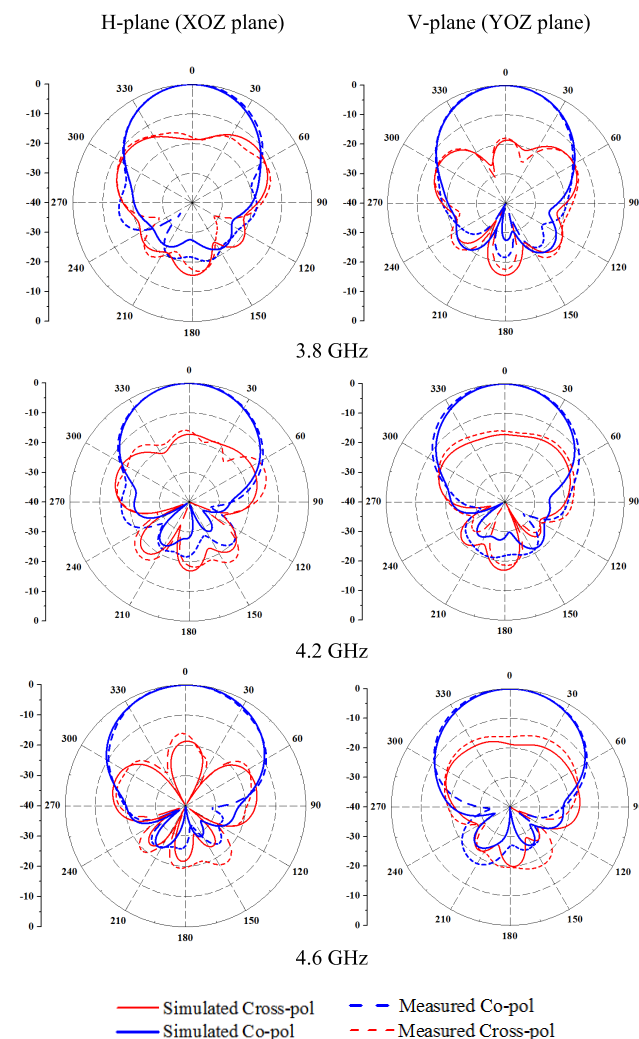


FIGURE 14. Performances of radiation pattern of the proposed CP ME dipole antenna over the operating frequencies.

C. DISCUSSION ON DIMENSION OF THE EBG SURFACE

In this section, the antenna performances of EBG surface with different dimensions are studied. Here, the LP ME dipole antenna is employed as the model to carry on investigation. The detailed diagrams and simulated performances have been shown in Fig. 15, Fig. 16, Fig. 17 and Fig. 18. Basically, the dimension of EBG structure can be described with two parameters of N_x and N_y , where N_x and N_y correspond to the number of the EBG unit along x direction and y direction, respectively. The simulated performances of SWR and FBR with different N_x are shown in Fig. 17. It can be seen that both the SWR and FBR are quite sensitive to the variation of N_x . When decreasing the number of N_x from 9 to 5, the FBR will be improved at lower frequencies and degraded at upper frequencies. The simulated SWR and FBR with different N_y are shown in Fig. 18. The SWR is quite stable with the change of N_y . When N_y increases from 5 to 9, the FBR over the entire operating frequencies will be enhanced. Therefore, the EBG surface can cause considerable effect on the E-planes than on the H-planes, and larger EBG surface can lead to improved

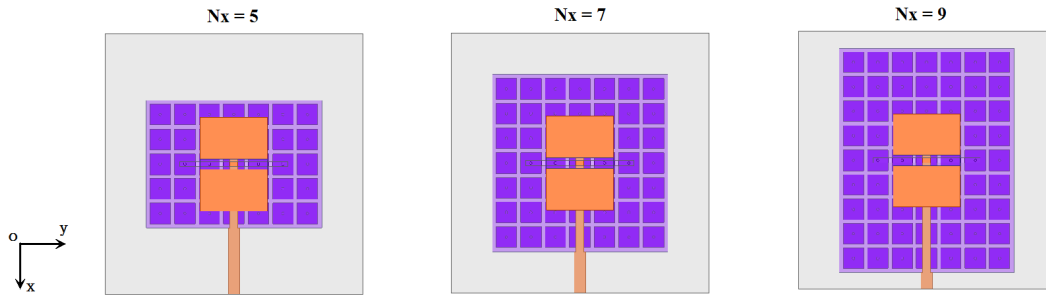


FIGURE 15. Proposed structure of aperture-coupled LP ME dipole antenna fed by microstrip line backed with EBG surface of different N_x .

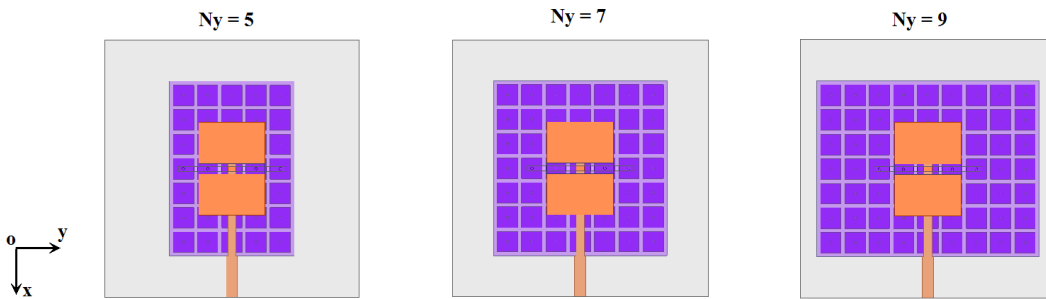


FIGURE 16. Proposed structure of aperture-coupled LP ME dipole antenna fed by microstrip line backed with EBG surface of different N_y .

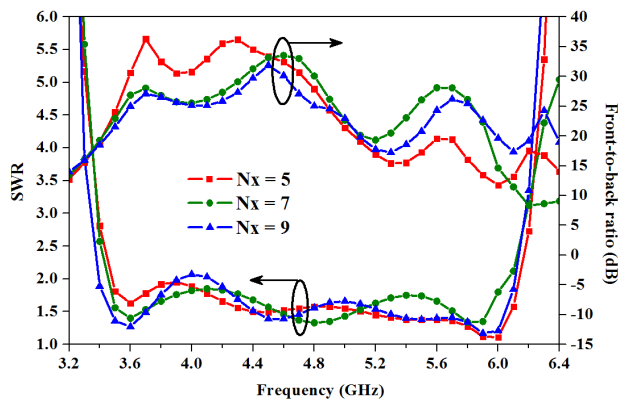


FIGURE 17. Simulated SWR and front-to-back ratio of the proposed LP ME dipole antenna backed with EBG surface of different N_x .

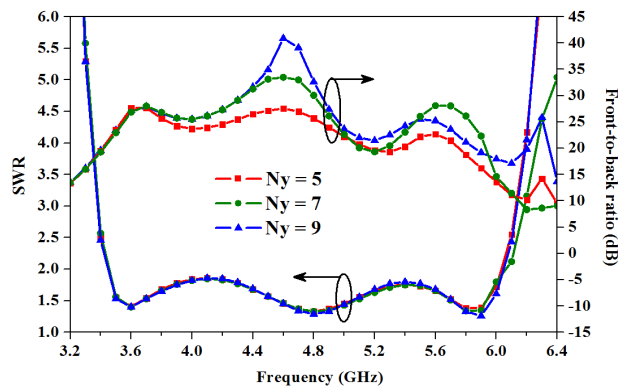


FIGURE 18. Simulated SWR and front-to-back ratio of the proposed LP ME dipole antenna backed with EBG surface of different N_y .

performances of the FBR. In terms of both the antenna cost and performances, a combination of larger N_x and moderate N_y is recommended.

VI. CONCLUSION

Aperture-coupled wideband magneto-electric dipole antennas excited by microstrip lines have been proposed in this paper. A printed electromagnetic bandgap (EBG) layer was mounted below the microstrip line to reduce the back radiations caused by the aperture. Both the feeding structure and the EBG layer can be realized using multiple PCBs, which is low in fabrication cost and ease of integration with other electronics or circuits. The aperture-coupled feeding method can effectively replace the conventional Γ -shaped probe, which is quite complicated and very sensitive to the antenna performance. Two prototypes of aperture-coupled ME dipoles with linear polarization and circular polarization have been designed and proposed. Both simulations and measurements were carried out for verification. The results turn out that both LP and CP ME dipole antennas fed by microstrip lines can achieve wide impedance bandwidth of over 50% with small back radiations. Besides, the realized gain and broadside radiation patterns are also very stable within respective operating frequencies.

ACKNOWLEDGMENT

Authors are very grateful to Mr. Chun Kwong LAU for his earnest assistance in the antenna fabrication.

REFERENCES

[1] J. G. Andrews *et al.*, "What will 5G be?" *IEEE J. Sel. Areas Commun.*, vol. 32, no. 6, pp. 1065–1082, Jun. 2014.

- [2] K.-F. Lee and K.-F. Tong, "Microstrip patch antennas—basic characteristics and some recent advances," *Proc. IEEE*, vol. 100, no. 7, pp. 2169–2180, Jul. 2012.
- [3] K. M. Luk, C. L. Mak, Y. L. Chow, and K. F. Lee, "Broadband microstrip patch antenna," *Electron. Lett.*, vol. 34, no. 15, pp. 1442–1443, Jul. 1998.
- [4] S. D. Targonski, R. B. Waterhouse, and D. M. Pozar, "Design of wideband aperture-stacked patch microstrip antennas," *IEEE Trans. Antennas Propag.*, vol. 46, no. 9, pp. 1245–1251, Sep. 1998.
- [5] S.-H. Wi, Y.-S. Lee, and J.-G. Yook, "Wideband microstrip patch antenna with U-shaped parasitic elements," *IEEE Trans. Antennas Propag.*, vol. 55, no. 4, pp. 1196–1199, Apr. 2007.
- [6] F. Yang, X.-X. Zhang, X. Ye, and Y. Rahmat-Samii, "Wide-band E-shaped patch antennas for wireless communications," *IEEE Trans. Antennas Propag.*, vol. 49, no. 7, pp. 1094–1100, Jul. 2001.
- [7] N.-W. Liu, L. Zhu, W.-W. Choi, and X. Zhang, "A low-profile aperture-coupled microstrip antenna with enhanced bandwidth under dual resonance," *IEEE Trans. Antennas Propag.*, vol. 65, no. 3, pp. 1055–1062, Mar. 2017.
- [8] I. Rana and N. Alexopoulos, "Current distribution and input impedance of printed dipoles," *IEEE Trans. Antennas Propag.*, vol. AP-29, no. 1, pp. 99–105, Jan. 1981.
- [9] P. Katehi and N. Alexopoulos, "On the effect of substrate thickness and permittivity on printed circuit dipole properties," *IEEE Trans. Antennas Propag.*, vol. AP-31, no. 1, pp. 34–39, Jan. 1983.
- [10] K.-L. Wong, F.-R. Hsiao, and T.-W. Chiou, "Omnidirectional planar dipole array antenna," *IEEE Trans. Antennas Propag.*, vol. 52, no. 2, pp. 624–628, Feb. 2004.
- [11] B. G. Duffley, G. A. Morin, M. Mikavica, and Y. M. M. Antar, "A wideband printed double-sided dipole array," *IEEE Trans. Antennas Propag.*, vol. 52, no. 2, pp. 628–631, Feb. 2004.
- [12] Q. Chu, D. Wen, and Y. Luo, "A Broadband $\pm 450^\circ$ dual-polarized antenna with Y-shaped Feeding Lines," *IEEE Trans. Antennas Propag.*, vol. 63, no. 2, pp. 483–490, Feb. 2015.
- [13] K. M. Luk and H. Wong, "A new wideband unidirectional antenna element," *Int. J. Microw. Opt. Technol.*, vol. 1, no. 1, pp. 35–44, Jun. 2006.
- [14] L. Ge and K. M. Luk, "A wideband magneto-electric dipole antenna," *IEEE Trans. Antennas Propag.*, vol. 60, no. 11, pp. 4987–4991, Nov. 2012.
- [15] Y. Li and K.-M. Luk, "60-GHz dual-polarized two-dimensional switch-beam wideband antenna array of aperture-coupled magneto-electric dipoles," *IEEE Trans. Antennas Propag.*, vol. 64, no. 2, pp. 554–563, Feb. 2016.
- [16] Y. Li and K.-M. Luk, "A 60-GHz wideband circularly polarized aperture-coupled magneto-electric dipole antenna array," *IEEE Trans. Antennas Propag.*, vol. 64, no. 4, pp. 1325–1333, Apr. 2016.
- [17] X. Cui, F. Yang, M. Gao, L. Zhou, Z. Liang, and F. Yan, "A wideband magneto-electric dipole antenna with microstrip line aperture-coupled excitation," *IEEE Trans. Antennas Propag.*, vol. 65, no. 12, pp. 7350–7354, Dec. 2017.
- [18] X. Cui, F. Yang, M. Gao, and Z. Liang, "Wideband microstrip magneto-electric dipole antenna with stripline aperture-coupled excitation," *IET Microw., Antennas Propag.*, vol. 12, no. 9, pp. 1575–1581, Mar. 2018.
- [19] D. Sievenpiper, L. Zhang, R. F. J. Broas, N. G. Alexopoulos, and E. Yablonovitch, "High-Impedance Electromagnetic Surfaces with a Forbidden Frequency Band," *IEEE Trans. Microw. Theory Techn.*, vol. 47, no. 11, pp. 2059–2074, Nov. 1999.
- [20] F. Yang and Y. Rahmat-Samii, *Electromagnetic Band Gap Structures in Antenna Engineering*. Cambridge, MA, USA: Cambridge Univ. Press, 2009.
- [21] J. D. Shumpert, W. J. Chappell, and L. P. B. Katehi, "Parallel-plate mode reduction in conductor-backed slots using electromagnetic bandgap substrates," *IEEE Trans. Microw. Theory Techn.*, vol. 47, no. 11, pp. 2099–2104, Nov. 1999.
- [22] F. Elek, R. Abhari, and G. V. Eleftheriades, "A uni-directional ring-slot antenna achieved by using an electromagnetic band-gap surface," *IEEE Trans. Antennas Propag.*, vol. 53, no. 1, pp. 181–190, Jan. 2005.
- [23] R. Abhari and G. V. Eleftheriades, "Metallo-dielectric electromagnetic bandgap structures for suppression and isolation of the parallel-plate noise in high-speed circuits," *IEEE Trans. Microw. Theory Techn.*, vol. 51, no. 6, pp. 1629–1639, Jun. 2003.
- [24] S. D. Targonski and R. B. Waterhouse, "Reflector elements for aperture and aperture coupled microstrip antennas," in *IEEE Antennas Propag. Soc. Int. Symp. Dig.*, Montreal Quebec, Canada, vol. 3, Jul. 1997, pp. 1840–1843.



JIE SUN (S'15) was born in Nanjing, Jiangsu, China. He received the B.S. degree from the Nanjing University of Science and Technology, Nanjing, in 2014. He is currently pursuing the Ph.D. degree in electronic engineering with the City University of Hong Kong, Hong Kong.

His current research interests include water patch antennas, liquid antennas, dense dielectric patch antennas, transparent antennas, and millimeter-wave antennas.

Mr. Sun was a recipient of the Best Student Paper Award in the 2017 IEEE International Workshop on Electromagnetics: Applications and Student Innovation Competition, held at University College London (UCL), London, U.K.



KWAI-MAN LUK (M'79–SM'94–F'03) received the B.Sc. (Eng.) and Ph.D. degrees in electrical engineering from The University of Hong Kong, in 1981 and 1985, respectively.

He joined the Department of Electronic Engineering, City University of Hong Kong, in 1985, as a Lecturer. Two years later, he moved to the Department of Electronic Engineering, The Chinese University of Hong Kong, where he spent four years. In 1992, he returned to the City University

of Hong Kong, where he served as the Head of the Department of Electronic Engineering, from 2004 to 2010, and the Director of the State Key Laboratory of Millimeter Waves, from 2008 to 2013, and is also a Chair Professor of electronic engineering. He has authored four books, 11 research book chapters, over 360 journal papers, and 250 conference papers. He received 10 U.S. and more than 10 PRC patents on the design of a wideband patch antenna with an L-shaped probe feed. His recent research interests include the design of patch antennas, magneto-electric dipole antennas, dense dielectric patch antennas, and open resonator antennas for various wireless applications.

Dr. Luk is a fellow of the U.K. Royal Academy of Engineering, Chinese Institute of Electronics, PRC, Institution of Engineering and Technology, U.K., Institute of Electrical and Electronics Engineers, USA, and Electromagnetics Academy, USA. He received the Japan Microwave Prize at the 1994 Asia Pacific Microwave Conference held in Chiba, in 1994, the Best Paper Award at the 2008 International Symposium on Antennas and Propagation held in Taipei, in 2008, and the Best Paper Award at the 2015 Asia-Pacific Conference on Antennas and Propagation held in Bali, in 2015. He received the very competitive 2000 Croucher Foundation Senior Research Fellow in Hong Kong, the 2011 State Technological Invention Award (second Honor) of China, and the recipient of the 2017 IEEE APS John Kraus Antenna Award. He was the Technical Program Chairperson of the 1997 Progress in Electromagnetics Research Symposium (PIERS), the General Vice Chairperson of the 1997 and 2008 Asia-Pacific Microwave Conference (APMC), the General Chairman of the 2006 IEEE Region Ten Conference (TENCON), the Technical Program Co-Chairperson of the 2008 International Symposium on Antennas and Propagation (ISAP), the General Co-Chairperson of the 2011 IEEE International Workshop on Antenna Technology (IWAT), the General Co-Chair of the 2014 IEEE International Conference on Antenna Measurements and Applications (CAMA), and the General Co-Chair of the 2015 International Conference on Infrared, millimeter, and Terahertz Waves (IRMMW-THz 2015). He is the General Chair of the 2020 Asia-Pacific Microwave Conference to be held in Hong Kong, in 2020. He was a Chief Guest Editor for a special issue on "Antennas in Wireless Communications" published in the Proceedings of the IEEE, in 2012. He is the Deputy Editor-in-Chief of PIERS journals and an Associate Editor of *IET Microwaves, Antennas and Propagation*.

• • •